Supplemental Information for

Human behavioral responses to climate change reshape climate projections

Yan Dou[1], Jialei Zhu[1*], Cong-qiang Liu[1]

[1] Institute of Surface-Earth System Science, School of Earth System Science, Tianjin University, Tianjin, China

*Corresponding author Email: zhujialei@tju.edu.cn

This PDF includes:

Texts S1-S8

References

Figures S1-S11

Tables S1-S4

Text S1 Parameter selection

To quantify the role of human behavioral processes in shaping climate–human feedbacks, we conduct a global sensitivity analysis on parameters governing the perception–emotion–behavior pathway and its interaction with climate signals. Parameters are selected to represent key stages of the modeled causal chain linking climate dynamics to behavioral responses: (i) climate signal generation (physical climate system), (ii) event exposure and memory formation (memory module), (iii) risk perception (perception process), and (iv) emotional and cognitive response system (Fig. 1). This framework is consistent with established theories of environmental risk perception and behavioral adaptation, which suggest that behavioral responses emerge through a sequence of perception, evaluation, emotional processing, and action rather than directly from physical climate change itself [1–7]. We select thirteen parameters that directly influence how climatic signals are translated into perceived risk, emotional response, and behavioral change. Parameter ranges were chosen based on previous empirical studies, theoretical considerations, and exploratory simulations to ensure coverage of plausible behavioral and climatic uncertainty.

The first group of parameters characterizes the generation and intensity of climate signals, which serve as the external drivers of perception, including two parameters. Extreme threshold (upper tail Threshold) determines the percentile threshold used to define an extreme event in the temperature distribution. Values between 0.95 and 0.99 correspond to widely used definitions of extremes based on the 95th–99th percentile of historical climate distributions[8–10]. Temperature Scale Factor adjusts the sensitivity of extreme event frequency to temperature change. The range (0.8–1.2) represents moderate uncertainty in the relationship between global warming and the occurrence of climate extremes consistent with evidence that warming generally increases the frequency and intensity of heat-related extreme events while substantial regional variability remains[8,11]. Within these ranges, a one-unit increase in each parameter corresponds to a proportional increase in the strength of climate hazard signals entering the perception system.

The second group of parameters governs how climate events are filtered, stored, and retained in human memory. Previous studies suggest that individuals respond primarily to remembered experiences rather than to the full set of observed climate events[10,12]. Three parameters control this process. Not all sensed extreme events are encoded into memory. The model therefore distinguishes between sensed extreme events and those retained in memory. Memory threshold determines the proportion of sensed climate events that are encoded into memory. The range $(0-1)$ reflects uncertainty in how individuals filter weak, ambiguous, or less salient environmental signals. Memory window defines the temporal window over which extreme events are accumulated in memory. The selected range (0.5–5 years) reflects empirical evidence suggesting that personal experience with extreme weather can influence risk perception for several years following the event[13–17]. The larger values of memory window correspond to longer period during which extreme events are sensed and potentially affect behavior. For example, increasing memory window by one year extends the time horizon over which past events contribute to perceived risk. Memory retention factor determines the persistence of remembered climate experiences. Larger values correspond to slower forgetting and longer retention times, whereas smaller values produce more rapid memory decay. The selected range (0.25–1.5) allows representation of both rapid attenuation and prolonged persistence of climate-event memories, consistent with studies of environmental memory and risk perception dynamics[18–20].

The third group of parameters describes how remembered climate experiences are translated into perceived climate risk. Consistent with risk-perception theory, perceived risk is represented as a combination of perceived severity and perceived susceptibility[21]. Norm events represent the reference level of remembered extreme events required to influence severity assessments. The range (5–20) is based on the variation in remembered extreme-event frequency generated by the coupled model and reflects uncertainty in the threshold at which climate experiences become psychologically salient. Perceived severity is also influenced by extreme intensity, which controls severity of individual remembered extreme events. remembered extreme events. The range of extreme intensity (0–1) represents variation in perceived event magnitude and its influence on risk evaluation. Perceived susceptibility is calculated by average affected population (global population *0.001) of extreme events, which is influenced by extreme intensity of extreme events in memory and intensity sensitivity. Intensity sensitivity determines how strongly event intensity affects perceived susceptibility through impacts on affected populations. The selected range (0–1) captures heterogeneity in individual sensitivity to information regarding climate impacts and exposure[22]. Severity weighting represents the relative weight assigned to perceived event severity compared with perceived susceptibility (personal exposure). Its range (0–1) allows the perception system to vary from exposure-dominated (Severity weighting close to 0) to severity-dominated (Severity weighting close to 1) risk evaluation. Increasing these parameters modifies the sensitivity of risk perception to environmental cues. For instance, increasing Severity weighting shifts the perception system toward greater emphasis on event severity rather than personal exposure. Perception delay represents the delay with which individuals update their perception of climate risk. The range (0.5–3 years) captures variability in how quickly populations respond to changing environmental signals[19,23]. Within the model, increasing these parameters alters the persistence and influence of past experiences on current risk perception.

The final group of parameters captures emotional and cognitive responses that mediate behavioral outcomes. PAC represents perceived self-efficacy, defined as an individual's belief in their ability to undertake effective climate-related actions[1,6,24–26]. CAC represents collective efficacy, defined as the belief that coordinated societal actions can effectively mitigate climate risks[1,27–29]. Both parameters range from 0.1 to 0.9, reflecting the distribution of efficacy beliefs commonly observed in behavioral studies, where extreme values near 0 or 1 are rare. Within the model, these two parameters are combined using the harmonic mean to represent overall efficacy, ensuring that low values in either component limit the resulting efficacy level. SCA represents the sensitivity of climate anxiety to perceived climate risk. Its range (0–1) captures variation in emotional responsiveness across individuals and populations[7,25,26,30,31]. A one-unit increase in SCA corresponds to a proportional increase in the translation of perceived threat into climate anxiety, while increases in efficacy parameters strengthen the likelihood that anxiety leads to pro-environmental behavior rather than maladaptive responses. This formulation is consistent with evidence that individuals differ substantially in the degree to which perceived climate threats evoke anxiety and climate-related distress[7,32,33].

Text S2 Methods for sensitivity and machine learning analyses

To quantify the relative importance of model parameters in driving variability in temperature outcomes, we employed a variance-based global sensitivity analysis using Sobol indices[34]. Sobol analysis is particularly suitable for nonlinear and interacting systems, as it does not rely on linear assumptions and allows for a comprehensive attribution of uncertainty across parameters.

This method decomposes the total variance of the model output into contributions attributable to individual parameters and their interactions.

Let $Y=f(X_1, X_2, ..., X_{13})$ denote the model output (temperature change), where $X_1, X_2, ..., X_{13}$ represents 13 input parameters. The total variance of the output is given by Var (Y).

The contribution of each parameter is quantified through variance decomposition. The first-order (S_i) contribution of parameter X_i, representing its independent effect, is defined as:

$$S_i = \frac{Var_{xi}(E\ [Y \mid X_i])}{Var(Y)}$$

The total contribution of X_i (ST), which includes both its direct effect and all interaction effects with other parameters, is given by:

$$S_{T_i} = 1 - \frac{Var_{X\sim i}(E\ [Y \mid X_{\sim i}])}{Var(Y)}$$

where $X_{\sim i}$ denotes all parameters except X_i. The total-effect index captures both the direct contribution of a parameter and all higher-order interaction effects involving that parameter. The difference between total (ST) and independent (S1) contributions therefore reflects the strength of interaction effects.

To complement the variance-based sensitivity analysis, we applied machine learning methods to evaluate the predictive importance of behavioral parameters. Specifically, we used random forest models and regression trees.

Regression trees estimate the relationship between input variables and temperature outcomes by repeatedly splitting the data into smaller and more homogeneous groups[18]. At each split, the algorithm selects the variable and threshold that minimize the variation of temperature within each group (measured as the sum of squared deviations from the group mean).

Random forest is an ensemble learning method that builds upon regression trees by aggregating a large number of decision trees constructed from bootstrap-resampled datasets[35]. During model training, each tree is fitted using a different subset of the simulation data, and at each split, a randomly selected subset of behavioral parameters is considered. This stochastic design reduces correlation among trees and enhances the robustness of predictions of temperature change. Final estimates of temperature change are obtained by averaging across all trees, which improves predictive reliability and reduces overfitting.

Variable importance is assessed using a permutation-based approach. For each behavioral parameter, its values are randomly permuted while all other parameters are held unchanged, and the resulting increase in prediction error of temperature change is evaluated. A larger increase in error indicates a stronger contribution of the parameter to explaining variability in projected temperature change. Importance is quantified as the percentage increase in prediction error, providing a standardized measure for comparing the relative influence of different behavioral parameters on temperature outcomes.

Text S3 Consistency of dominant behavior drivers across emission scenarios

To evaluate whether the dominant behavioral controls identified under SSP5-8.5 remain robust across alternative emissions pathways, we extend the Sobol sensitivity (Fig. 3) and random forest analyses (Figure S3) to SSP1-2.6 and SSP2-4.5 (Tables S2–S4). Across all scenarios, the same small subset of behavioral parameters consistently dominates projected temperature outcomes, indicating that the overall structure of behavioral influence is largely independent of the background emissions trajectory.

Sobol analysis shows that PAC and CAC exert the strongest independent effects (S1) and combined effects (ST) across all scenarios and time horizons (Table S2). Under SSP1-2.6, both parameters maintain nearly identical contributions in 2050 and 2100, with S1 values around 0.40 and ST values around 0.48. Under SSP2-4.5, their direct effects decrease from approximately 0.37 in 2050 to 0.29 in 2100, while combined effects decline from approximately 0.49 to 0.41. A similar reduction occurs under SSP5-8.5, where the combined effect of PAC and CAC decrease from 0.46 in 2050 to 0.38 and 0.36 in 2100, respectively. Despite these reductions, PAC and CAC remain the two largest contributors to temperature variability in every scenario, highlighting the persistent importance of cognitive adjustment processes in regulating climate–behavior feedbacks.

In contrast, the contribution of SCA exhibits a strong dependence on both emissions pathway and time horizon. Under SSP1-2.6, the independent effect of SCA remains nearly unchanged between 2050 and 2100 (S1= 0.03), whereas its combined effect increases from 0.06 to0.10, suggesting that interactions involving climate anxiety become more important over time even when its independent contribution remains stable. Under SSP2-4.5, both direct and combined effects increase substantially, with independent effect rising from 0.05 to 0.11 and ST increasing from 0.09 to 0.20. The strongest increase occurs under SSP5-8.5, where the independent effect of SCA increases more than sixfold, from 0.03 in 2050 to 0.22 in 2100, while its combined effect increases from 0.12 to 0.34. By 2100 under SSP5-8.5, the independent effect of SCA (0.22) becomes comparable to those of PAC (0.23) and CAC (0.27), indicating that climate anxiety evolves from a relatively minor contributor into one of the principal determinants of long-term temperature variability under high-emissions conditions. Although the relative importance of individual parameters changes across scenarios, the overall sensitivity structure remains highly concentrated. The six most influential behavioral parameters—PAC, CAC, SCA, memory window, memory retention factor, and severity weighting—collectively explain 94.4–97.1% of total model sensitivity across all scenario–year combinations (Table S3). Consequently, the remaining seven parameters account for less than 6% of total sensitivity despite representing multiple aspects of memory dynamics, risk perception, and extreme-event characterization. This concentration indicates that uncertainty propagation within the coupled climate–human system is governed primarily by a limited set of behavioral mechanisms, resulting in an effective behavioral dimensionality that is substantially lower than the total number of model parameters.

Random forest analysis provides independent support for this conclusion. Across all scenarios, PAC, CAC, and SCA consistently rank as the three most important predictors of projected temperature change (Table S4; Figure S3). Together, these three parameters account for 73.58% and 74.85% of total predictive importance under SSP1-2.6 in 2050 and 2100, respectively, 72.48% and 76.24% under SSP2-4.5, and 70.54% and 80.99% under SSP5-8.5. Among all variables, SCA is the only parameter that exhibits a systematic increase in predictive importance across both time horizons and emissions pathways. Its relative contribution increases from 20.74% to 22.58% under SSP1-2.6, from 24.36% to 30.41% under SSP2-4.5, and from 24.73% to 33.41% under SSP5-8.5. This pattern closely mirrors the trend observed in the Sobol analysis, indicating that the growing influence of climate anxiety is robust across both variance-based and prediction-based assessment methods.

The Sobol and random forest analyses reveal a consistent behavioral hierarchy across all emissions scenarios. PAC and CAC remain the dominant behavioral controls throughout the century, whereas the influence of SCA strengthens progressively from SSP1-2.6 to SSP5-8.5 and from 2050 to 2100. These results suggest that long-term temperature outcomes are governed by a highly concentrated subset of behavioral mechanisms and that the relative importance of emotional responses increases as climate change intensifies, eventually approaching that of cognitive adjustment processes under high-emissions futures.

Text S4 Regression tree analysis of behavioral controls on divergent temperature outcomes

The regression tree analysis provides a mechanistic interpretation of how behavioral uncertainty generates divergent temperature trajectories in the coupled climate–behavior system (Figure S5). While the Sobol and random forest analyses identify the behavioral parameters contributing most strongly to temperature variability, the regression trees reveal how specific combinations of these parameters produce distinct warming and cooling pathways.

Across all emission scenarios, the range of temperature outcomes relative to the no-response baseline expands substantially from 2050 to 2100. Under SSP1-2.6, temperature deviations range from −0.16 °C to +0.65 °C in 2050 but widen to −0.14 °C to +2.41 °C by 2100. Under SSP2-4.5, the corresponding range expands from −0.29 °C to +0.55 °C in 2050 to −0.73 °C to +2.46 °C in 2100. The largest divergence occurs under SSP5-8.5, where outcomes span −0.42 °C to +0.60 °C in 2050 and expand dramatically to −2.10 °C to +2.76 °C in 2100. Consistent with Figure S4, both the magnitude of temperature deviations and the proportion of simulations reaching extreme states increase over time. Under SSP5-8.5, for example, the strongest warming increases from +0.79 °C (7.4% of simulations) in 2050 to +2.76 °C (16.7%) in 2100, while the strongest cooling intensifies from −0.53 °C (19.8%) to −2.10 °C (30.2%). These patterns indicate that behavioral uncertainty exerts an increasingly strong influence on long-term climate trajectories.

The structure of the regression trees shows that this divergence is governed primarily by three behavioral parameters: collective action capacity (CAC), personal action capacity (PAC), and sensitivity of climate anxiety (SCA). Across all scenarios, these variables consistently occupy the upper levels of the trees and define the major branching points separating warming and cooling trajectories, whereas severity weighting appears mainly in lower-order branches and the remaining parameters contribute little to the overall tree architecture. This pattern closely mirrors the Sobol and random forest analyses, which identify PAC, CAC, and SCA as the dominant contributors to temperature variability across all emission pathways.

The organization of behavioral controls changes substantially between 2050 and 2100. In all three scenarios, CAC forms the root split in 2050, indicating that collective efficacy acts as the primary determinant of behavioral divergence during the mid-century period. This finding is consistent with social-cognitive theories that identify collective efficacy as a key prerequisite for coordinated climate action, particularly when mitigation outcomes depend on collective rather than individual efforts[36,37]. Under SSP1-2.6, high CAC (⩾ 0.35) generally constrains temperature deviations and produces slight cooling (−0.16 °C), whereas lower CAC values lead to warming branches reaching +0.65 °C. Similar CAC-centered structures are observed under SSP2-4.5 and SSP5-8.5, where PAC and SCA further partition the system into alternative warming and cooling trajectories. In these mid-century trees, extreme outcomes emerge only when multiple behavioral conditions align simultaneously, indicating that large temperature responses remain dependent on relatively complex interactions among efficacy beliefs and emotional responses.

By 2100, the control structure becomes increasingly concentrated around a smaller set of dominant behavioral thresholds. Under SSP1-2.6, the root split shifts from CAC to PAC, indicating that individual efficacy becomes the primary organizing factor of system dynamics. Under SSP2-4.5 and SSP5-8.5, SCA emerges as the root node (threshold = 0.5), separating trajectories that subsequently evolve toward substantially different climate outcomes. The increasing prominence of climate-anxiety sensitivity is consistent with evidence that emotional responses become increasingly influential as climate risks become more frequent, personally experienced, and psychologically salient[31,38]. The emergence of SCA at the highest level of the trees is also consistent with the sensitivity analyses, which show a progressive increase in both its direct effect (S1) and combined effect (ST), particularly under SSP2-4.5 and SSP5-8.5 by 2100.

The pathways associated with extreme warming and cooling become increasingly differentiated by the end of the century. Under SSP5-8.5, the strongest cooling outcome (−2.10 °C) occurs when SCA ⩾ 0.5, CAC ⩾ 0.25, and PAC ⩾ 0.25, indicating that strong emotional engagement with climate risks is translated into effective behavioral responses through both collective and individual efficacy. In contrast, the strongest warming outcome (+2.76 °C) emerges under low SCA (< 0.5), low PAC (< 0.35), and weaker collective efficacy. This pattern suggests that concern about climate change alone is insufficient to alter climate trajectories; rather, emotional responses become most effective when accompanied by strong beliefs in both personal and collective response capacity. Such interactions are consistent with Protection Motivation Theory and related efficacy-based models of environmental behavior, which emphasize that risk perception promotes adaptive action primarily when effective responses are perceived to be available[21,39]. Similar SCA-centered bifurcations characterize SSP2-4.5, where cooling reaches −0.73 °C and warming reaches +2.46 °C, while SSP1-2.6 exhibits a weaker but qualitatively consistent transition toward PAC- and SCA-dominated controls.

The regression tree results demonstrate that behavioral uncertainty influences not only the magnitude of future temperature change but also the structure of possible climate trajectories. The dominant branching variables identified by the trees correspond closely to those highlighted by the Sobol and random forest analyses, providing independent evidence that PAC, CAC, and SCA constitute the primary behavioral controls of long-term climate outcomes. The convergence of these results across multiple analytical approaches supports the growing recognition that behavioral feedbacks can substantially alter projected climate trajectories and should be explicitly represented in climate–human system models[18,40]. As the century progresses, differences in efficacy beliefs and climate-anxiety sensitivity increasingly determine whether the coupled system follows relatively cool or substantially warmer pathways, particularly under intermediate- and high-emission futures.

Text S5 Cumulative impact of behavioral response timing on temperature trajectories under SSP1-2.6 and SSP2-4.5 scenario

Under both SSP1-2.6 and SSP2-4.5 scenarios, the projected 2100 temperature response consistently increases when coupled human behavioral responses are initiated earlier, indicating a robust cumulative effect of intervention timing across forcing levels. When decomposed relative to the no-response baselines (1.60°C for SSP1-2.6 and 2.40°C for SSP2-4.5), both warming above the baseline and cooling below the baseline exhibit systematic dependence on the start time of behavioral coupling.

For SSP1-2.6, the warming component increases from +0.71°C (P25–P75) for a 2030 start, to +1.16°C for 2020, and +1.53°C for 2010, corresponding to additional warming of 0.82°C and 0.37°C when comparing 2010 with 2030 and 2020, respectively. The cooling component similarly strengthens from −0.13°C (2030) to −0.22°C (2020) and −0.31°C (2010), indicating progressively enhanced cooling effects with earlier intervention.

In SSP2-4.5, the same pattern persists but with larger absolute magnitudes: warming increases from +1.42°C (2030), to +1.72°C (2020), and +1.96°C (2010), while cooling intensifies from −0.71°C (2030) to −0.84°C (2020) and −0.94°C (2010). These results demonstrate that earlier behavioral activation consistently amplifies both positive (cooling-enhancing) and negative (warming-enhancing) feedbacks, while delayed or prolonged maladaptive responses allow warming-related feedbacks to accumulate more strongly over time. Notably, although SSP2-4.5 exhibits stronger overall feedback magnitudes than SSP1-2.6, the direction and timing-dependent structure of the response remain consistent across scenarios. The consistency of this pattern across emission scenarios indicates that the influence of behavioral processes depends not only on on the length of time over which they interact with the climate system but also their direction. Earlier activation allows both adaptive and maladaptive behavioral responses to accumulate over a longer period, resulting in progressively larger cooling and warming deviations by 2100. These findings provide additional evidence that climate–behavior interactions are fundamentally cumulative processes, and that the timing of behavioral change can be as important as its magnitude in shaping long-term climate trajectories.

Text S6 Alternative emission adjustment formulation

To assess the robustness of the behavioral-emissions coupling formulation, we implement an alternative discrete adjustment scheme for emissions dynamics. In this specification, fossil fuel CO_2 emissions are updated using a bounded stepwise correction rather than a continuous differential formulation.

Baseline emissions E are obtained from SSP scenarios. After a coupling start time (2010), emissions are adjusted according to behavioral influence as follows:

$$E^{*} = \begin{cases} \qquad\qquad\qquad E, & t < t_{start} \\ \max(E_{min}, \quad E + \Delta E, & t \geq t_{start} \end{cases}$$

where the behavioral adjustment term is defined as:

$$\Delta E = \alpha * (E - E_{min}) * Emissions\ Intensity\ Factor$$

With:

$$Emissions\ Intensity\ Factor = -BehaviorChange$$

Here, α represents the maximum annual emissions adjustment rate (0.5/yr), and E_{min} is the lower-bound emission constraint (5 GtCO2/yr). The formulation ensures that emissions remain physically bounded while allowing behavioral feedback to modulate emissions proportionally to the remaining reducible emissions space $(\mathrm{E} - \mathrm{E}_{\mathrm{min}})$.

The continuous formulation conceptualizes (used in the main text) behavioral influence as a gradual and continuously evolving process, in which emissions respond smoothly over time to changes in behavior. This representation reflects a system-level view in which behavioral shifts are progressively translated into emissions changes through continuous adjustments in consumption patterns, technology adoption, and policy implementation. In contrast, the alternative formulation represents behavioral influence as a more discrete and stepwise process, in which behavioral changes are translated into emissions adjustments at distinct time intervals. This interpretation is closer to real-world decision-making and policy processes, where changes in emissions often occur through periodic interventions, regulatory updates, or sectoral transitions rather than as a fully continuous adjustment. The key conceptual distinction between the two approaches lies in the temporal granularity of behavioral feedback transmission.

The continuous formulation assumes that behavioral effects are continuously integrated into the emissions system, resulting in smooth trajectory adjustments over time. The discrete formulation, on the other hand, assumes that the same behavioral influence is realized in a more episodic manner, where its effects are periodically expressed in the emissions trajectory.

Despite these differences in temporal representation, both formulations are built on the same core mechanism: behavioral change modifies emissions in proportion to the remaining emissions reduction potential and is constrained by a lower bound representing structural limits in hard-to-abate sectors. This shared structure ensures that emissions responses remain bounded and physically interpretable under both approaches. Importantly, the consistency between the two formulations indicates that the qualitative system behavior is not sensitive to whether behavioral feedback is represented as a continuous or discrete process. Instead, the dynamics are primarily driven by the strength and direction of the behavioral coupling itself, rather than the specific mathematical implementation of its temporal expression. This provides evidence that the modeled relationship between human behavior and emissions trajectories is structurally robust under alternative representations of feedback timing.

Text S7 Robustness of behavioral–emissions coupling to alternative temporal representations

To assess the robustness of the behavioral–emissions coupling formulation, we compare temperature outcomes derived from the alternative level-based adjustment of emissions, in which behavioral feedback directly modifies emission levels, with those obtained from the rate-based dynamic adjustment used in the main text, in which behavioral feedback modulates the rate of emissions change over time.

Despite this fundamental difference in implementation, both approaches produce qualitatively consistent temperature responses across SSP scenarios. In both formulations, behavioral feedback leads to scenario-dependent deviations from the baseline, with stronger mitigation effects under high-emission pathways (SSP5–8.5) and more modest responses under lower-emission scenarios (SSP1–2.6 and SSP2–4.5). The magnitude of end-of-century temperature changes remains broadly comparable between the two approaches, indicating that the overall climate response is not sensitive to the specific mathematical representation of behavioral feedback.

To further evaluate the robustness of the behavioral–emissions coupling and the influence of temporal integration, we compare the sensitivity of temperature outcomes to human behavioral parameters under the level-based adjustment (direct emissions modifications) and the rate-based dynamic adjustment (emissions rate modifications) across SSP scenarios at 2050 and 2100 (Figure S9-S10). In all scenarios, cognitive and emotional adjustment parameters (PAC, CAC, SCA) dominate the variance contribution, while memory-related parameters (memory window, memory retention factor, severity weighting) contribute moderately.

Under SSP5–8.5, both formulations identify PAC and CAC as the top contributors in 2050, with independent effects accounting for the majority of variance. The rate-based adjustment, however, exhibits a stronger cumulative influence of SCA by 2100, reflecting the path-dependent accumulation of behavioral effects, whereas in the level-based formulation, SCA remains relatively minor and its impact largely stems from interactions with other parameters.

For SSP2–4.5, the dominant behavioral drivers are consistent across formulations, but the rate-based approach shows larger contributions from SCA at 2100, indicating that cumulative dynamics amplify the effect of late-acting cognitive and emotional responses. Under SSP1–2.6, differences between formulations are more pronounced at 2050: in the level-based adjustment, SCA contributes minimally, whereas in the rate-based adjustment, SCA is elevated due to the integration of early behavioral effects. By 2100, both formulations converge in terms of dominant parameters, though rate-based adjustment maintains slightly higher independent contributions from SCA.

These comparisons illustrate that while the qualitative ranking of dominant behavioral parameters is robust, the magnitude of contributions—especially for SCA—is sensitive to whether behavioral feedback is applied instantaneously or through cumulative rate-based dynamics. Furthermore, early versus late introduction of behavioral feedback has little effect under level-based adjustments but substantially alters cumulative contributions under rate-based adjustments, highlighting the importance of temporal integration for the amplification of adaptive or maladaptive behaviors. Although RF importance rankings at 2050 under the discrete adjustment method show a slightly different order, the cumulative variance over longer horizons confirms that PAC, CAC, and SCA remain the dominant drivers. The transient differences reflect the stepwise propagation of behavioral feedback in the discrete model.

To further connect the sensitivity analysis with the temporal dynamics of behavioral feedback, we examine how the timing of behavioral coupling influences cumulative climate outcomes. Consistent with the results presented in the main text, the impact of behavioral feedback on temperature trajectories depends critically on whether its effects are integrated over time.

Under the level-based adjustment, where behavioral feedback directly modifies emissions levels without accumulation, the timing of behavioral intervention has a negligible effect on long-term temperature outcomes (Figure S11). Early and late coupling produce nearly identical cumulative impacts, indicating that instantaneous adjustments do not generate significant path dependence.

In contrast, under the rate-based dynamic adjustment, behavioral feedback operates on the rate of emissions change and accumulates over time, leading to pronounced timing sensitivity (Fig. 4). Earlier coupling results in substantially larger cumulative effects, amplifying both warming driven by maladaptive behaviors and cooling driven by adaptive responses. This reflects the integration of behavioral influence along the emissions trajectory, whereby small early differences are progressively magnified through feedback dynamics.

These results reinforce the central conclusion of the main text: the long-term impact of human behavior on climate outcomes is governed not only by the direction and magnitude of behavioral change, but also by how its effects accumulate over time, with early interventions playing a disproportionately important role under dynamically evolving emissions systems.

Text S8 Dynamic Psychological activation thresholds

Behavior responses in the model are governed by activation thresholds for climate anxiety and perceived efficacy. CAthreshold defines the threshold above which climate anxiety is considered high. Effthreshold defines the threshold above which efficacy is considered high. Both parameters range from 0.5 to 1, reflecting the assumption that strong emotional or efficacy responses only occur above moderate perception levels. Thresholds are constructed by two approaches: evolved with societal baselines derived from historical data and fixed[13].

The climate anxiety threshold is estimated using two empirical proxies: language-based index constructed using Google Books Ngram frequencies of climate- and anxiety-related terms[41,42], and disaster exposure index derived from EM-DAT records of climate-related disasters (droughts, floods, storms, temperature extremes and wildfires). Parallelly, the efficacy constructed by language-based collective action index derived from Google Books Ngram frequencies associated with environmental activism, behavior change, and climate policy discourse, combined with global education rate data as a structural proxy for cognitive capacity and social empowerment[43]. Each series is normalized and expressed relative to its 1850 baseline. Where sufficient data points are available, logistic functions are fitted to historical trajectories to represent long-term diffusion dynamics of social concern. In cases of insufficient data, linear extrapolation is applied. The projected series are normalized to a 0–1 range and combined using weighted averaging to produce a composite climate anxiety proxy. Rolling window percentiles (10 years) are then computed to generate percentile-based activation thresholds (P50, P75, P90), allowing behavioral activation to depend on historically evolving social baselines rather than fixed cut-offs.

References

1. Bradley, G. L., Babutsidze, Z., Chai, A. & Reser, J. P. The role of climate change risk perception, response efficacy, and psychological adaptation in pro-environmental behavior: A two nation study. *J. Environ. Psychol.* **68**, 101410 (2020).
2. Doherty, K. L. & Webler, T. N. Social norms and efficacy beliefs drive the Alarmed segment's public-sphere climate actions. *Nat. Clim. Change* **6**, 879–884 (2016).
3. Ajzen, I. Perceived Behavioral Control, Self-Efficacy, Locus of Control, and the Theory of Planned Behavior[1]. *J. Appl. Soc. Psychol.* **32**, 665–683 (2002).
4. Van Valkengoed, A. M. & Steg, L. Meta-analyses of factors motivating climate change adaptation behaviour. *Nat. Clim. Change* **9**, 158–163 (2019).
5. Clayton, S. *et al.* Psychological research and global climate change. *Nat. Clim. Change* **5**, 640–646 (2015).
6. Beckage, B., Moore, F. C. & Lacasse, K. Incorporating human behaviour into Earth system modelling. *Nat. Hum. Behav.* **6**, 1493–1502 (2022).
7. Innocenti, M. *et al.* How Can Climate Change Anxiety Induce Both Pro-Environmental Behaviours and Eco-Paralysis? The Mediating Role of General Self-Efficacy. *Int. J. Environ. Res. Public. Health* **20**, 3085 (2023).
8. Intergovernmental Panel On Climate Change (Ipcc). *Climate Change 2021 – The Physical Science Basis: Working Group I Contribution to the Sixth Assessment Report of the Intergovernmental Panel on Climate Change*. (Cambridge University Press, 2023). doi:10.1017/9781009157896.
9. Fischer, E. M. & Knutti, R. Anthropogenic contribution to global occurrence of heavy-precipitation and high-temperature extremes. *Nat. Clim. Change* **5**, 560–564 (2015).
10. Howe, P. D., Boudet, H., Leiserowitz, A. & Maibach, E. W. Mapping the shadow of experience of extreme weather events. *Clim. Change* **127**, 381–389 (2014).
11. Intergovernmental Panel On Climate Change (Ipcc). *Climate Change 2021 – The Physical Science Basis: Working Group I Contribution to the Sixth Assessment Report of the Intergovernmental Panel on Climate Change*. (Cambridge University Press, 2023). doi:10.1017/9781009157896.
12. Lieder, F., Griffiths, T. L. & Hsu, M. Overrepresentation of extreme events in decision making reflects rational use of cognitive resources. *Psychol. Rev.* **125**, 1–32 (2018).
13. Weber, E. U. Experience-Based and Description-Based Perceptions of Long-Term Risk: Why Global Warming does not Scare us (Yet). *Clim. Change* **77**, 103–120 (2006).
14. Ai, X., Han, Z. & Zhang, Q. Extreme weather experience and climate change risk perceptions: The roles of partisanship and climate change cause attribution. *Int. J. Disaster Risk Reduct.* **108**, 104511 (2024).
15. Dablander, F. Climate hazard experience linked to increased climate risk perception worldwide. *Environ. Res. Lett.* **20**, 114010 (2025).
16. Kroher, L. & Hoffmann, R. Harbingers of climate change: The role of extreme weather experiences in perceiving and acting against climate change.
17. Sambrook, K., Konstantinidis, E., Russell, S. & Okan, Y. The Role of Personal Experience and Prior Beliefs in Shaping Climate Change Perceptions: A Narrative Review. *Front. Psychol.* **12**, 669911 (2021).
18. Beckage, B. *et al.* Linking models of human behaviour and climate alters projected climate

change. *Nat. Clim. Change* **8**, 79–84 (2018).

19. Egan, P. J. & Mullin, M. Turning Personal Experience into Political Attitudes: The Effect of Local Weather on Americans' Perceptions about Global Warming. *J. Polit.* **74**, 796–809 (2012).
20. Weber, E. U. What shapes perceptions of climate change? New research since 2010. *WIREs Clim. Change* **7**, 125–134 (2016).
21. Witte, K. Fear control and danger control: A test of the extended parallel process model (EPPM). *Commun. Monogr.* **61**, 113–134 (1994).
22. Intergovernmental Panel On Climate Change (Ipcc). *Climate Change 2022 – Impacts, Adaptation and Vulnerability: Working Group II Contribution to the Sixth Assessment Report of the Intergovernmental Panel on Climate Change*. (Cambridge University Press, 2023). doi:10.1017/9781009325844.
23. Zaval, L., Keenan, E. A., Johnson, E. J. & Weber, E. U. How warm days increase belief in global warming. *Nat. Clim. Change* **4**, 143–147 (2014).
24. Bandura, A. Self-efficacy: Toward a unifying theory of behavioral change. *Adv. Behav. Res. Ther.* **1**, 139–161 (1978).
25. Pasquariello, R., Donizzetti, A. R., Curcio, C., Capasso, M. & Caso, D. From Values to Action: The Roles of Green Self-Identity, Self-Efficacy, and Eco-Anxiety in Predicting Pro-Environmental Behaviours in the Italian Context. *Sustainability* **17**, 6838 (2025).
26. Poortinga, W., Demski, C. & Steentjes, K. Generational differences in climate-related beliefs, risk perceptions and emotions in the UK. *Commun. Earth Environ.* **4**, 229 (2023).
27. Moore, F. C. *et al.* Determinants of emissions pathways in the coupled climate–social system. *Nature* **603**, 103–111 (2022).
28. Bamberg, S., Rees, J. & Seebauer, S. Collective climate action: Determinants of participation intention in community-based pro-environmental initiatives. *J. Environ. Psychol.* **43**, 155–165 (2015).
29. Hornsey, M. J., Harris, E. A., Bain, P. G. & Fielding, K. S. Meta-analyses of the determinants and outcomes of belief in climate change. *Nat. Clim. Change* **6**, 622–626 (2016).
30. Cunsolo, A. *et al.* Ecological grief and anxiety: the start of a healthy response to climate change? *Lancet Planet. Health* **4**, e261–e263 (2020).
31. Ogunbode, C. A. *et al.* Climate anxiety, wellbeing and pro-environmental action: correlates of negative emotional responses to climate change in 32 countries. *J. Environ. Psychol.* **84**, 101887 (2022).
32. Baroni, M., Valdrighi, G., Guazzini, A. & Duradoni, M. "More than a Feeling": How Eco-Anxiety Shapes Pro-Environmental Behaviors and the Role of Readiness to Change. *Sustainability* **17**, 6154 (2025).
33. Carasso Romano, G. H., Sippori, R. & Soroker, S. Examining the relationship between ecological anxiety and pro-environmental behavior: personal and collective actions. *Front. Psychol.* **16**, 1505564 (2025).
34. Sobol′, I. M. Global sensitivity indices for nonlinear mathematical models and their Monte Carlo estimates. *Math. Comput. Simul.* **55**, 271–280 (2001).
35. Breiman, L. Random Forests. *Mach. Learn.* **45**, 5–32 (2001).
36. Bandura, A. Exercise of Human Agency Through Collective Efficacy. *Curr. Dir. Psychol. Sci.* **9**, 75–78 (2000).
37. Van Zomeren, M., Spears, R. & Leach, C. W. Experimental evidence for a dual pathway model

analysis of coping with the climate crisis. *J. Environ. Psychol.* **30**, 339–346 (2010).

38. Clayton, S. & Karazsia, B. T. Development and validation of a measure of climate change anxiety. *J. Environ. Psychol.* **69**, 101434 (2020).
39. Maddux, J. E. & Rogers, R. W. Protection motivation and self-efficacy: A revised theory of fear appeals and attitude change. *J. Exp. Soc. Psychol.* **19**, 469–479 (1983).
40. Eker, S., Reese, G. & Obersteiner, M. Modelling the drivers of a widespread shift to sustainable diets. *Nat. Sustain.* **2**, 725–735 (2019).
41. Andrew, J. H. *How Culture Shapes the Climate Change Debate*. (Stanford University Press, 2015).
42. Michel, J.-B. *et al.* Quantitative Analysis of Culture Using Millions of Digitized Books. *Science* **331**, 176–182 (2011).
43. Leiserowitz, A., Kotcher, J., Rosenthal, S., Goddard, E., Carman, J., Verner, M., Myers, T., Ettinger, J., Fine, J., Richards, E., Goldberg, M., Marlon, J., & Maibach, E. *Climate Change in the American Mind: Beliefs & Attitudes, Fall 2025*.

Figures

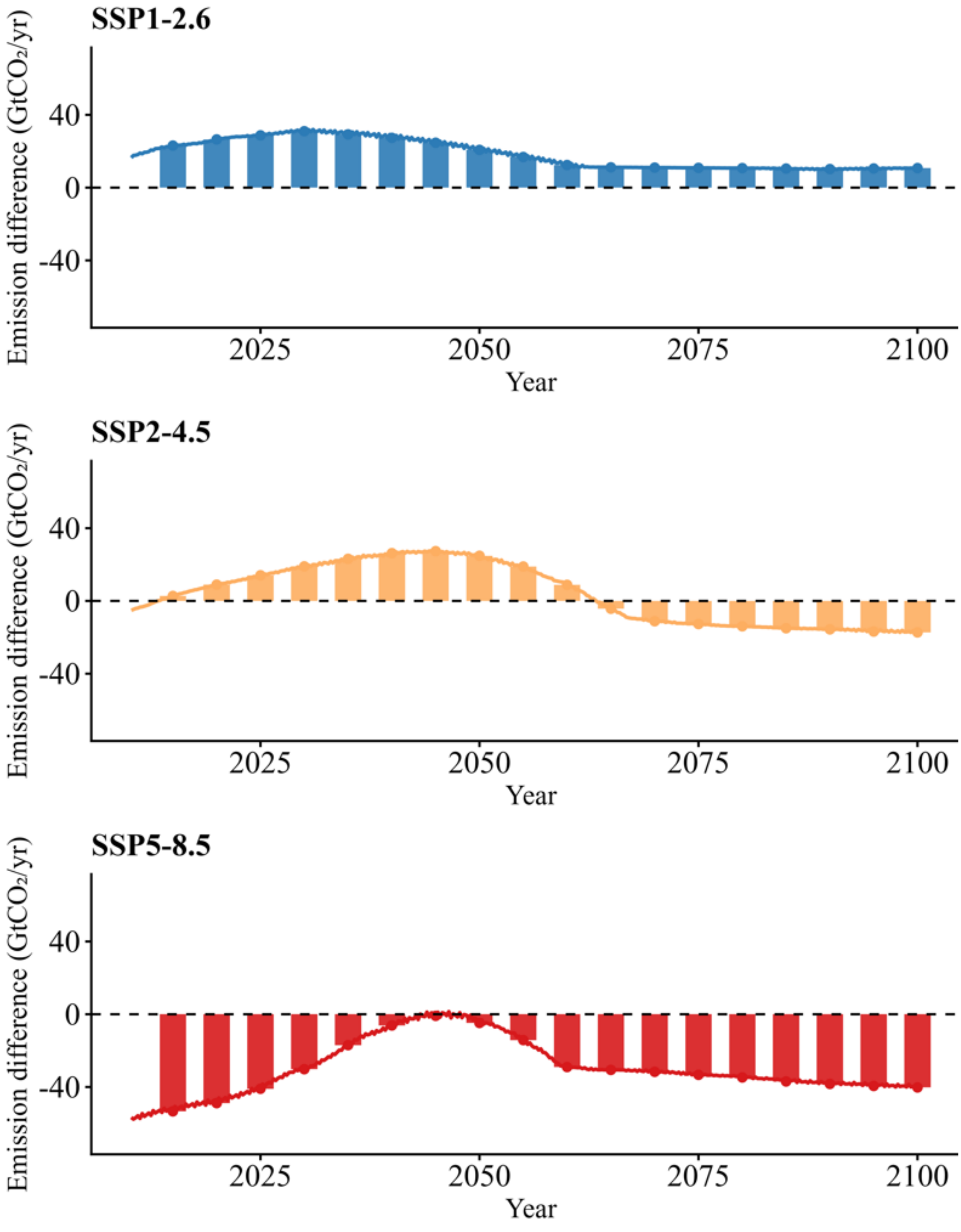

Figure S1. Changes in median emissions including behavioral responses relative to no-response baseline between 2010 and 2100 under different scenarios. Median emissions are shown at 5-year intervals under SSP1-2.6 (blue), SSP2-4.5 (orange) and SSP5-8.5 (red).

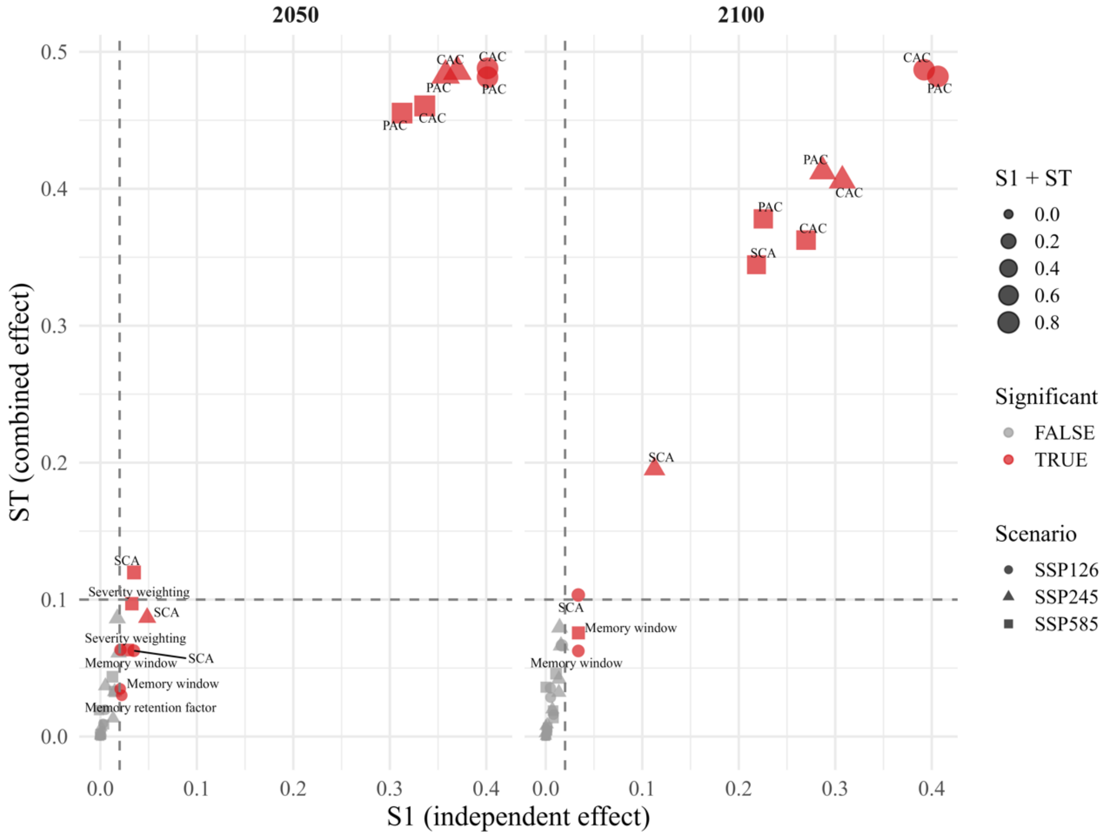

Figure S2 Selected parameters (red markers) based on Sobol sensitivity indices, using thresholds of independent effect (S1) > 0.02 and combined effect (ST) > 0.1. Parameters are retained if they satisfy the criteria in any time–scenario combination. S1 quantifies the individual contribution of a parameter to output variance (independent effect), whereas ST captures its total contribution, including interactions with other parameters (combined effect). Higher Sobol indices indicate greater influence on model variance.

(a)

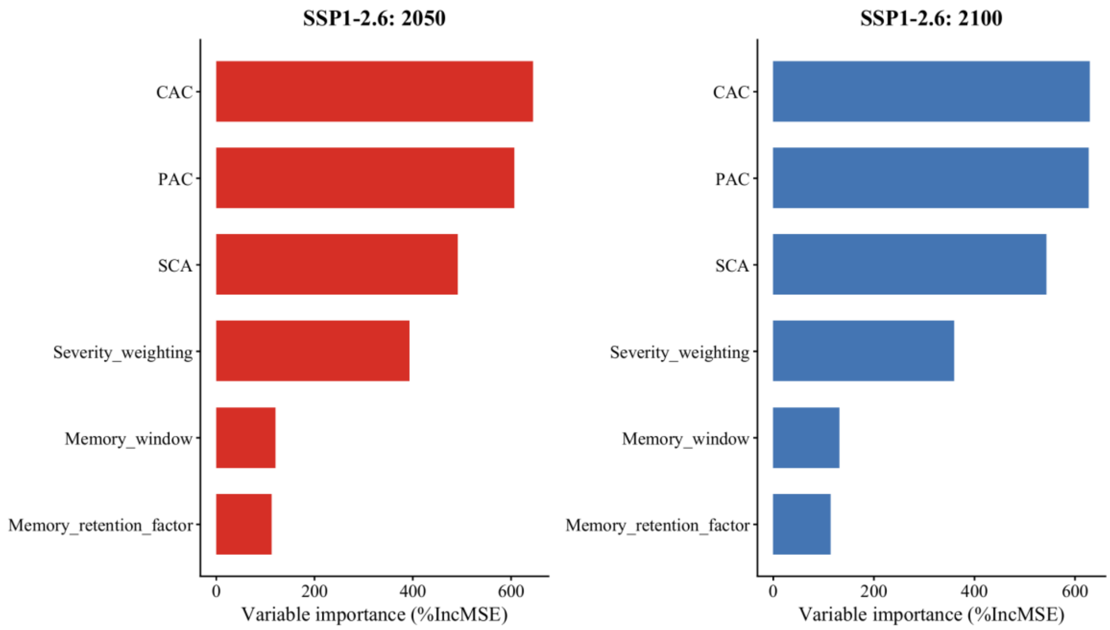
SSP1-2.6: 2050
CAC
PAC
SCA
Severity_weighting
Memory_window
Memory_retention_factor
0
200
400
600
Variable importance (%IncMSE)
SSP1-2.6: 2100
CAC
PAC
SCA
Severity_weighting
Memory_window
Memory_retention_factor
0
200
400
600
Variable importance (%IncMSE)

(b)

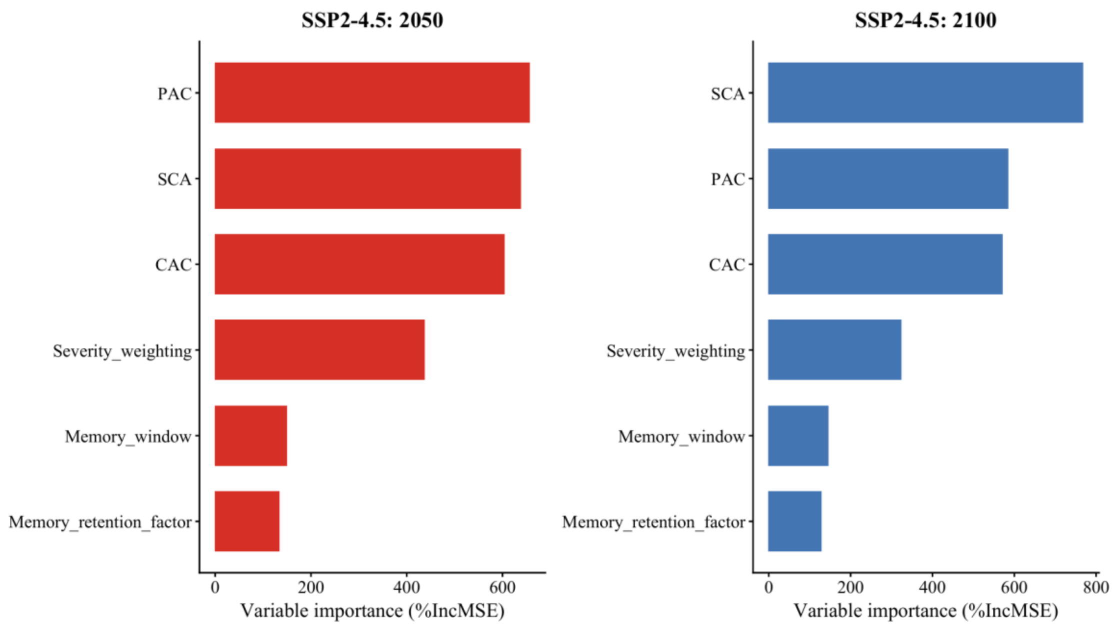
SSP2-4.5: 2050
PAC
SCA
CAC
Severity_weighting
Memory_window
Memory_retention_factor
0
200
400
600
Variable importance (%IncMSE)
SSP2-4.5: 2100
SCA
PAC
CAC
Severity_weighting
Memory_window
Memory_retention_factor
0
200
400
600
800
Variable importance (%IncMSE)

(c)

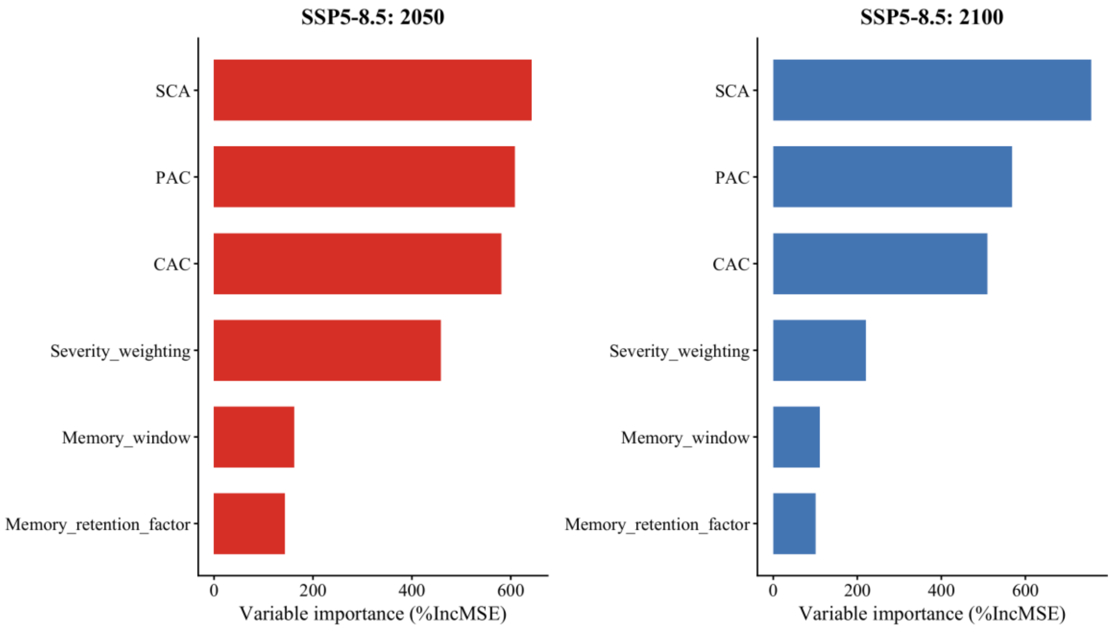

Figure S3. Random forest based variable importance across emission scenarios in 2050 and 2100. Importance is estimated using a random forest model for SSP1-2.6 (a), SSP2-4.5 (b) and SSP5-8.5 (c). Red and blue bars represent 2050 and 2100, respectively. Importance is measured as %IncMSE based on permutation loss in a 500-tree random forest. Seven Sobol-selected predictors are included.

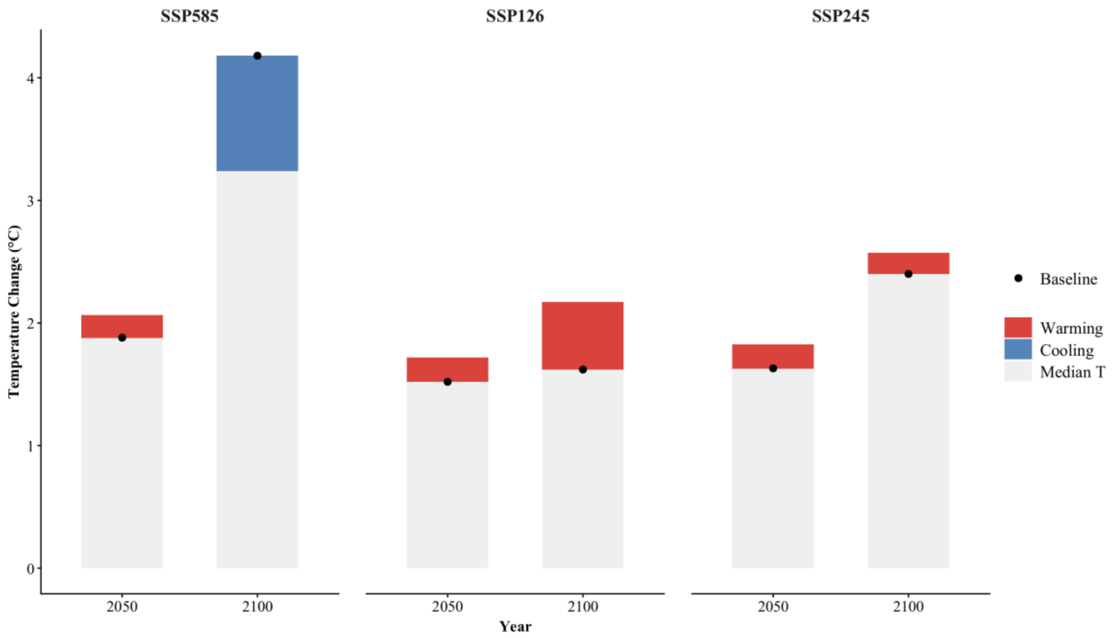

Figure S4 Temperature change due to behavioral responses relative to no-response baseline across scenarios and coupling assumptions. Median temperature change relative to no-response baseline comparison between 2050 and 2100 under different scenarios. Black dots represent no-response baseline. Deviations above the baseline are shown in red, and deviations below the baseline in blue

(a)

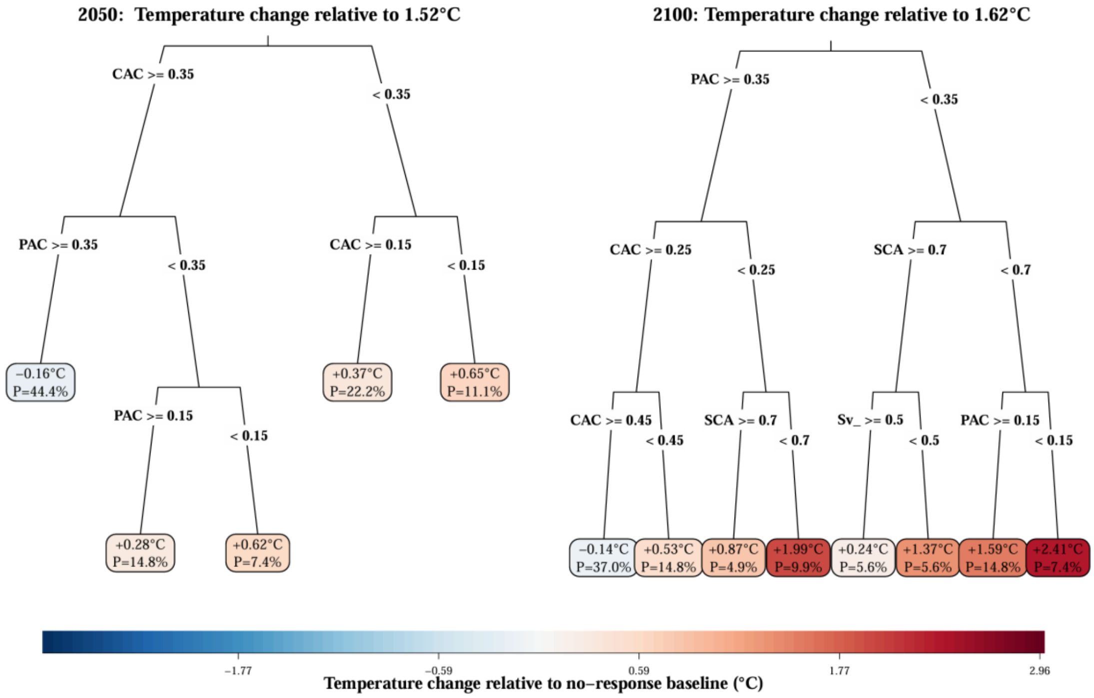
2050: Temperature change relative to 1.52°C
CAC >= 0.35
< 0.35
PAC >= 0.35
< 0.35
CAC >= 0.15
< 0.15
−0.16°C P=44.4%
PAC >= 0.15
< 0.15
+0.37°C P=22.2%
+0.65°C P=11.1%
+0.28°C P=14.8%
+0.62°C P=7.4%
2100: Temperature change relative to 1.62°C
PAC >= 0.35
< 0.35
CAC >= 0.25
< 0.25
SCA >= 0.7
< 0.7
CAC >= 0.45
< 0.45
SCA >= 0.7
< 0.7
Sv_ >= 0.5
< 0.5
PAC >= 0.15
< 0.15
−0.14°C P=37.0%
+0.53°C P=14.8%
+0.87°C P=4.9%
+1.99°C P=9.9%
+0.24°C P=5.6%
+1.37°C P=5.6%
+1.59°C P=14.8%
+2.41°C P=7.4%
−1.77
−0.59
0.59
1.77
2.96
Temperature change relative to no−response baseline (°C)

(b)

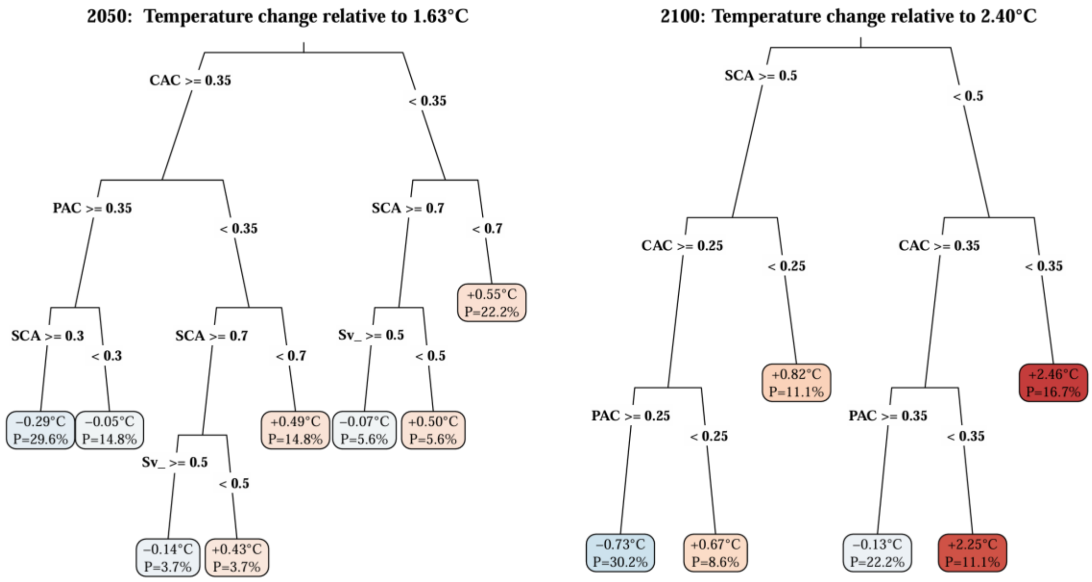
2050: Temperature change relative to 1.63°C
CAC >= 0.35
< 0.35
PAC >= 0.35
< 0.35
SCA >= 0.7
< 0.7
+0.55°C P=22.2%
SCA >= 0.3
< 0.3
SCA >= 0.7
< 0.7
Sv_ >= 0.5
< 0.5
−0.29°C P=29.6%
−0.05°C P=14.8%
+0.49°C P=14.8%
−0.07°C P=5.6%
+0.50°C P=5.6%
Sv_ >= 0.5
< 0.5
−0.14°C P=3.7%
+0.43°C P=3.7%
2100: Temperature change relative to 2.40°C
SCA >= 0.5
< 0.5
CAC >= 0.25
< 0.25
CAC >= 0.35
< 0.35
+0.82°C P=11.1%
+2.46°C P=16.7%
PAC >= 0.25
< 0.25
PAC >= 0.35
< 0.35
−0.73°C P=30.2%
+0.67°C P=8.6%
−0.13°C P=22.2%
+2.25°C P=11.1%

(c)

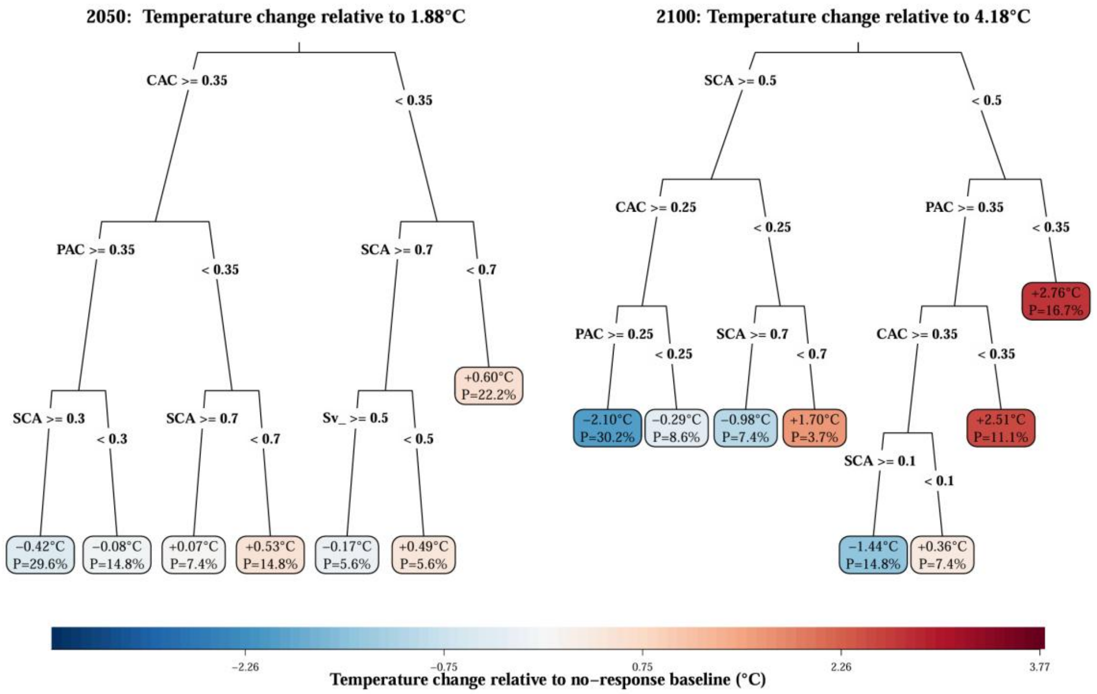

Figure S5. Regression tree of temperature change due to behavioral responses relative to no-response baseline in 2050 and 2100 under SSP1-2.6 (a), SSP2-4.5 (b), and SSP5-8.5 (c). Decision tree regression models are used to quantify the influence of behavioral and perception-related parameters, as well as temperature change from preindustrial levels, on temperature deviations from the baseline. The response variable is the temperature deviation relative to the no-response baseline, with baseline values of 1.52 °C (2050) and 1.62 °C (2100) for SSP1-2.6, 1.63 °C and 2.40 °C for SSP2-4.5, and corresponding values for SSP5-8.5. Blue (red) colors indicate decreases (increases) in temperature relative to the baseline, with color intensity representing the magnitude of deviation, scaled by the global maximum absolute deviation across all scenarios. Each node reports the mean temperature deviation and the proportion of samples within that node.

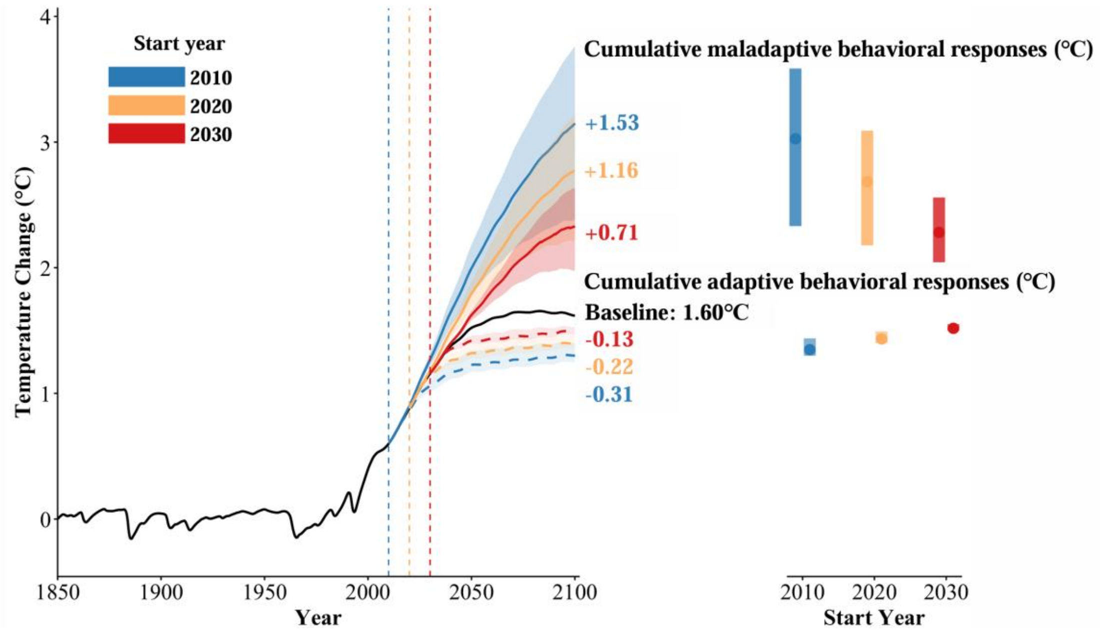

Figure S6. Temperature trajectories with a different start year (2010, 2020, 2030) of coupling human responses under SSP1-2.6 scenario. The left panel shows temperature change relative to a no-response baseline (black line prior to 2010). Total response is decomposed into above-baseline (solid lines) and below-baseline (dashed lines) components. Above-baseline and below-baseline components represent warming and cooling contributions relative to the no-response baseline. Colors indicate start year (blue: 2010; orange: 2020; red: 2030). The right panel shows corresponding temperature deviations in 2100.

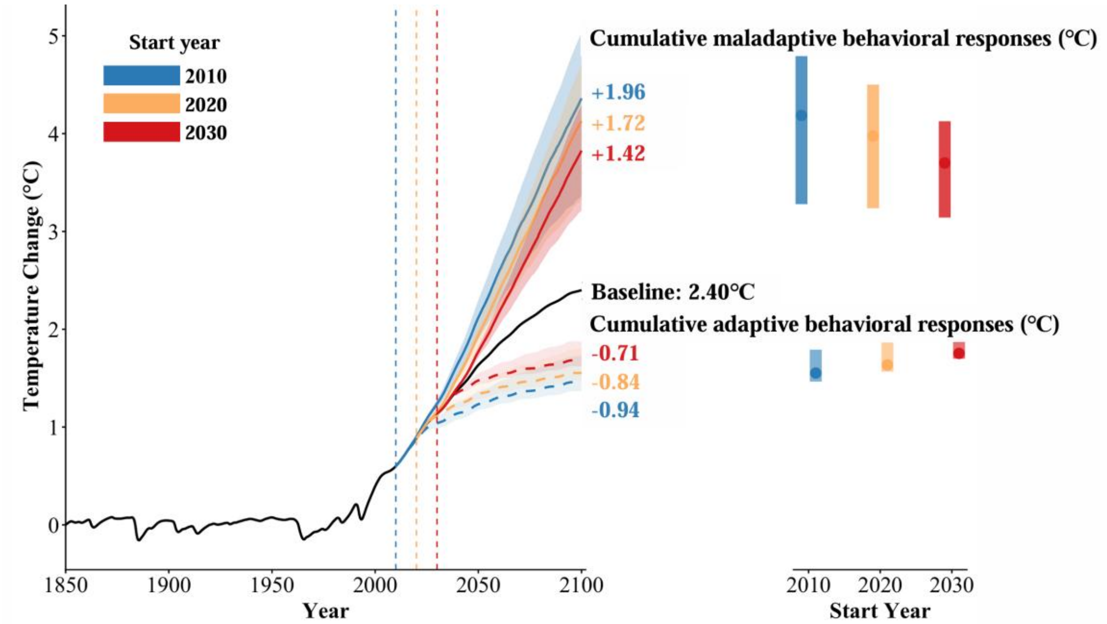

Figure S7. Temperature trajectories with a different start year (2010, 2020, 2030) of coupling human responses under SSP2-4.5 scenario. The left panel shows temperature change relative to a no-response baseline (black line prior to 2010). Total response is decomposed into above-baseline (solid lines) and below-baseline (dashed lines) components. Colors indicate start year (blue: 2010; orange: 2020; red: 2030). The right panel shows corresponding temperature deviations in 2100.

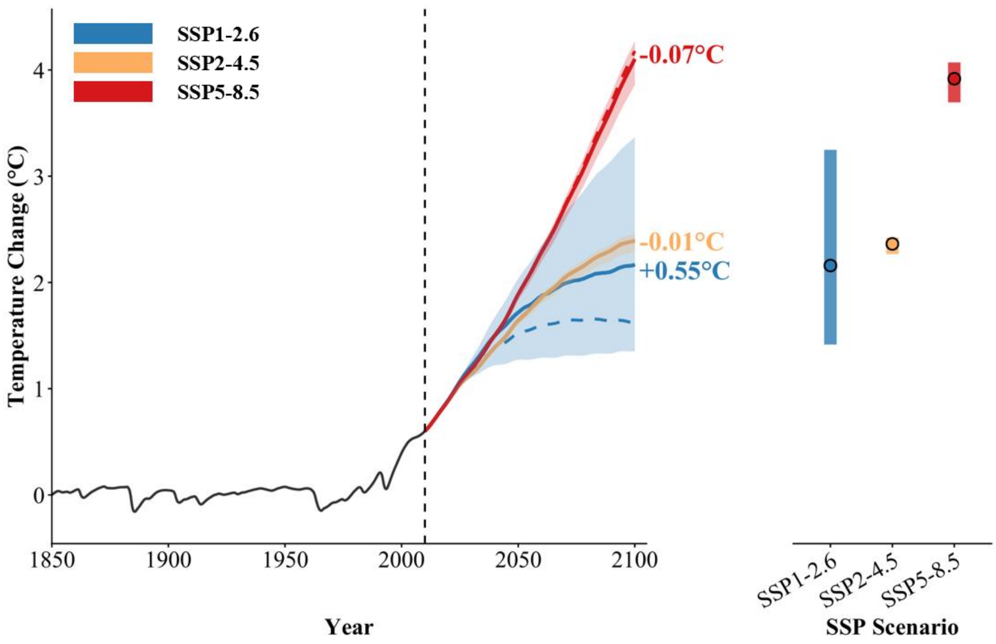

Figure S8 Temperature trajectories under direct adjustment of emissions by human behavior across SSP scenarios. The left panel shows global mean temperature change relative to the 1850 baseline. Before 2010, all scenarios follow the no-response baseline (black line). After 2010, colored dashed lines represent the continuation of the baseline without behavioral feedback, while colored solid lines show temperature trajectories when human behavior directly adjusts emissions at each time step. Results are shown for SSP1–2.6 (blue), SSP2–4.5 (orange), and SSP5–8.5 (red), with shaded areas indicating the interquartile range (25th–75th percentiles). Annotated values indicate the deviation of median temperature (P50) from the corresponding baseline. The right panel summarizes temperature outcomes in 2100, where black circled markers denote median values and colored bars represent the interquartile range. In this representation, behavioral changes are translated into immediate adjustments in emissions levels without accumulating over time. As a result, temperature deviations from the baseline remain relatively small and show limited sensitivity to the timing of behavioral responses. Compared to the gradual adjustment shown in Fig. 2, this direct adjustment approach produces weaker amplification of both warming and cooling effects, highlighting the importance of cumulative processes in shaping long-term climate outcomes.

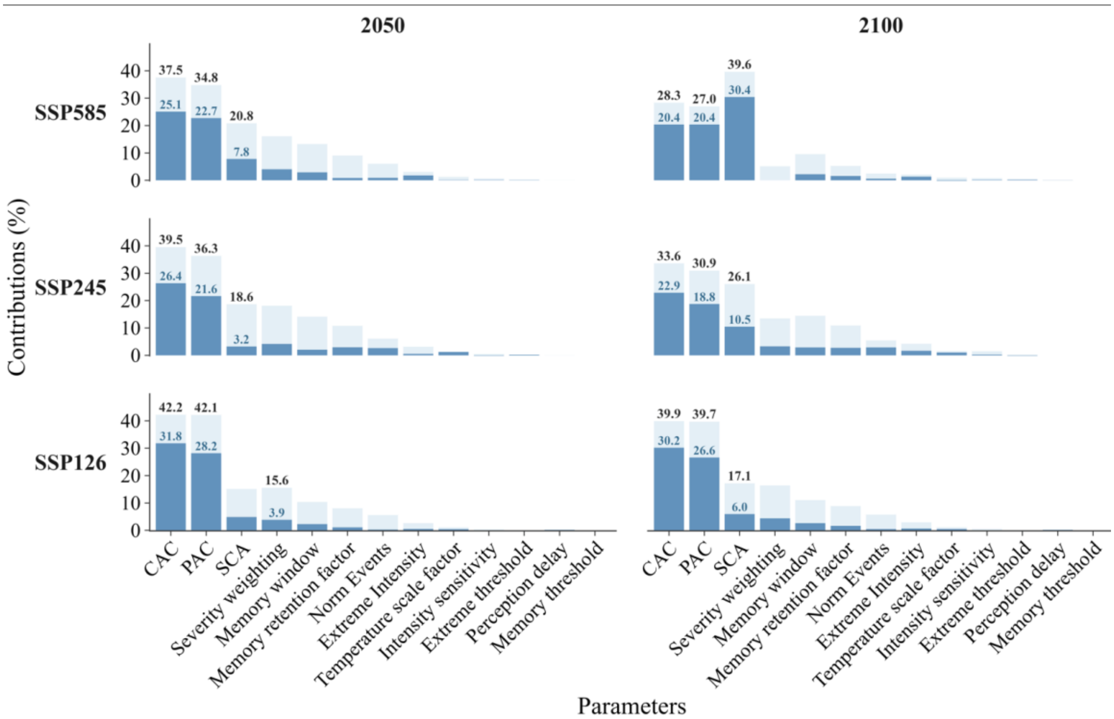

Figure S9 Sensitivity of projected temperature to human behavioral parameters under direct emissions adjustments across SSP scenarios. Contributions of 13 behavioral parameters to temperature variability are quantified using Sobol global sensitivity analysis under SSP5–8.5, SSP2–4.5, and SSP1–2.6 for 2050 and 2100. Light blue bars denote combined effects (ST), while dark blue segments indicate independent effects (S1). Across all scenarios and time horizons, PAC, CAC, and SCA dominate the variance contribution, with memory window, memory retention factor, and severity weighting also playing significant roles.

(a) SSP1-2.6

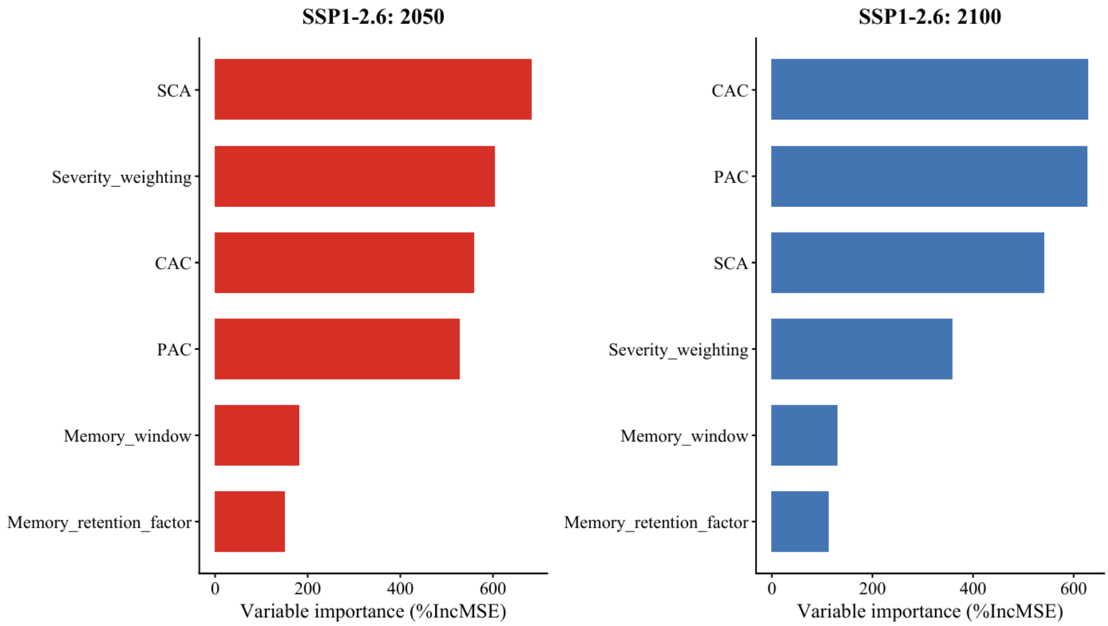

(b) SSP2-4.5

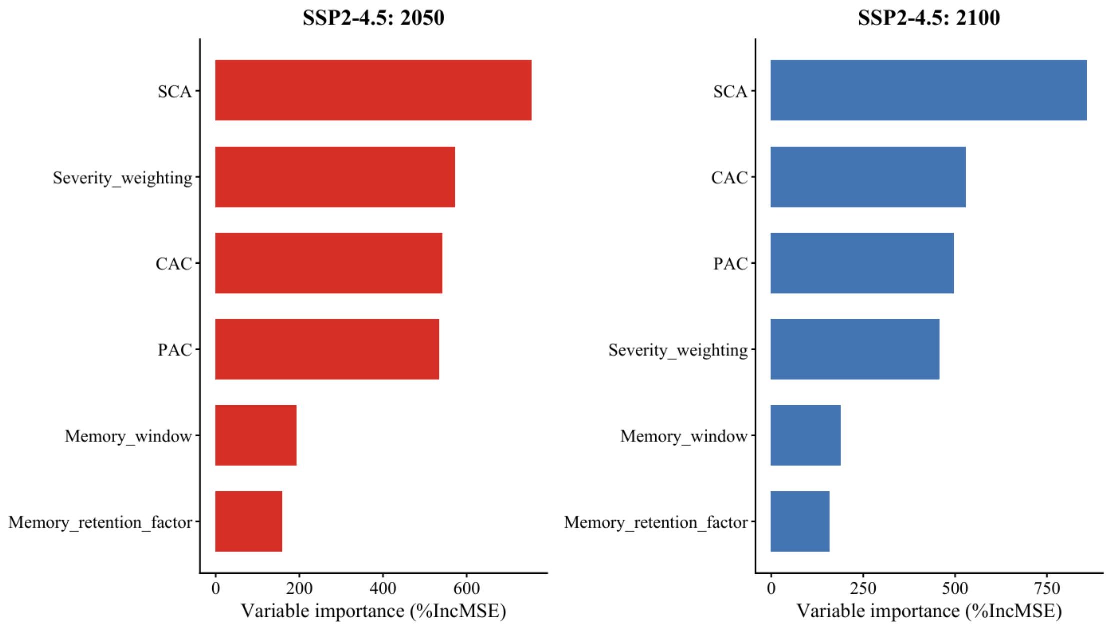

(c) SSP585

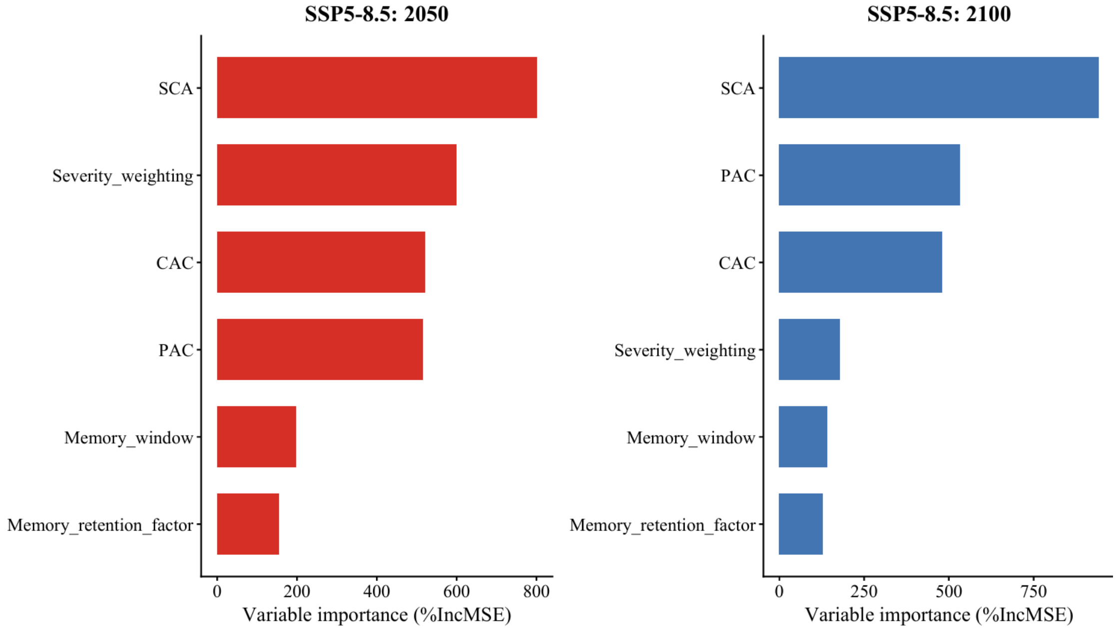

Figure S10. Random forest based variable importance under direct emission adjustments across emission scenarios in 2050 and 2100. Importance is estimated using a random forest model for SSP1-2.6 (a), SSP2-4.5 (b) and SSP5-8.5 (c). Red and blue bars represent 2050 and 2100, respectively. Importance is measured as %IncMSE based on permutation loss in a 500-tree random forest. Seven Sobol-selected predictors are included.

(a) SSP1-2.6

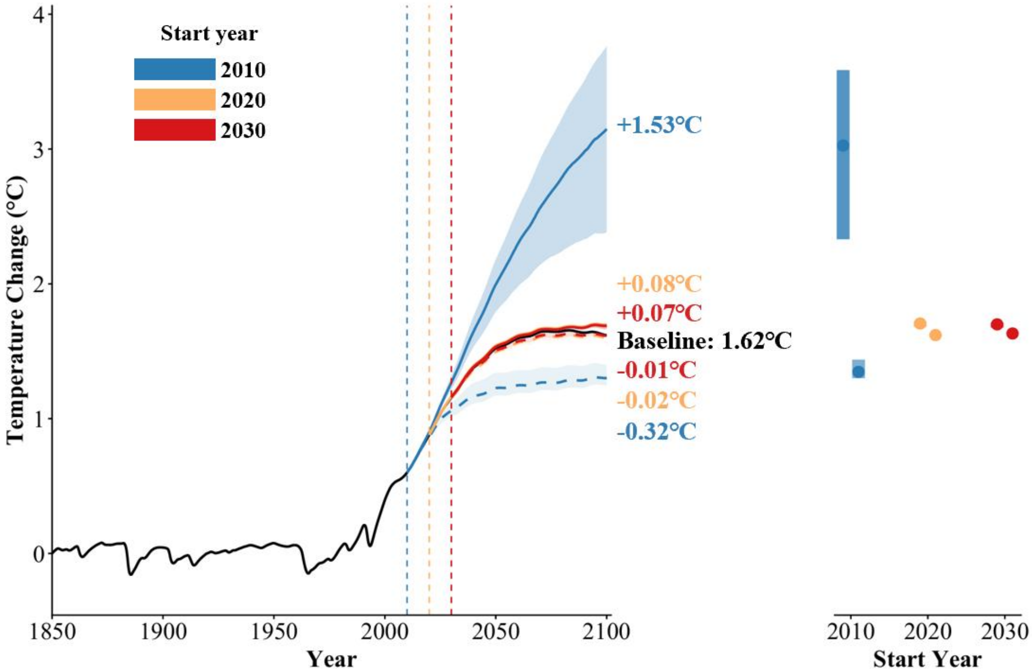

(b) SSP2-4.5

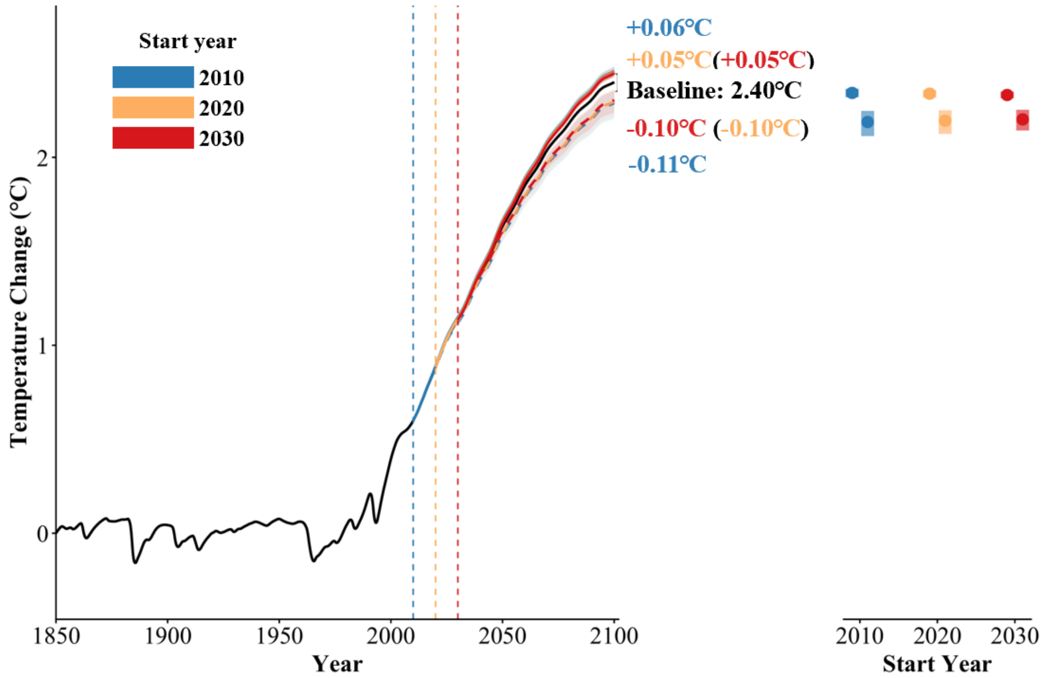

(c) SSP5-8.5

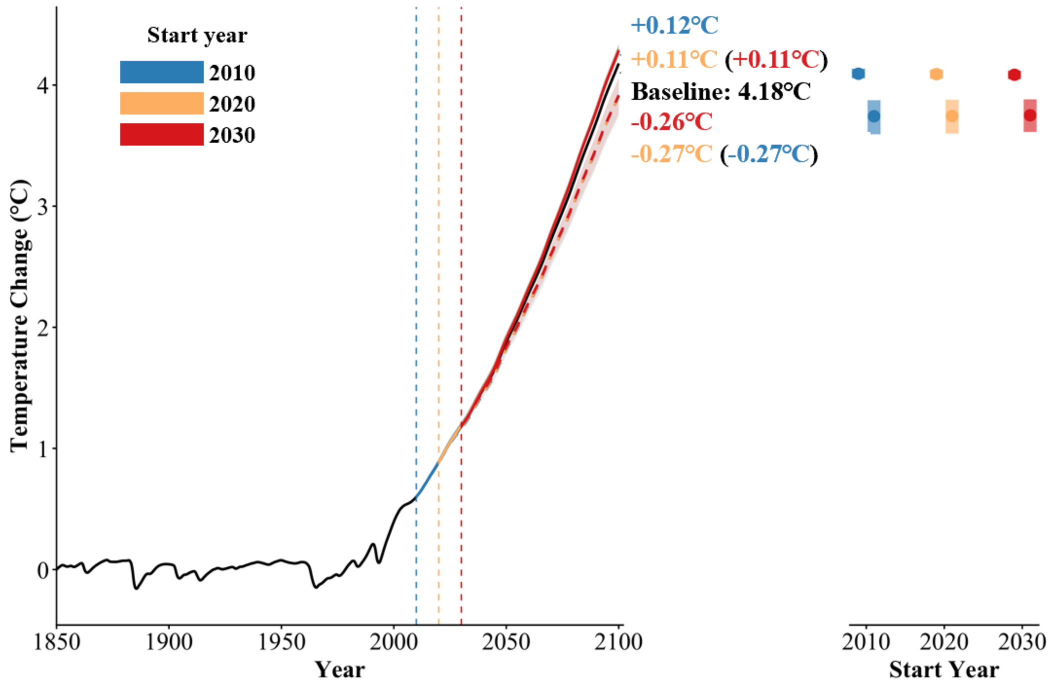

Figure S11. Warming and cooling trajectories with different behavioral coupling start year (2010, 2020,2030) under (a) SSP1–2.6, (b) SSP2–4.5, (c) SSP5–8.5. Solid lines show global mean temperature trajectories under direct emissions adjustment coupling, with intervention starting in 2010 (blue), 2020 (orange), and 2030 (red). Shaded bands indicate the uncertainty range associated with behavioral response. Right-hand panels display the corresponding end-of-century temperature changes relative to the baseline (no behavioral feedback). Early intervention produces the largest temperature reduction across all scenarios, with diminishing effectiveness for later start dates.

Supplementary Tables

Table S1 Parameter values and their uncertainty ranges.

System Domain	Parameter	Baseline	Min	Max	Description	Interpretation
Physical Climate System	Extreme threshold	0.98	0.95	0.99	Defines rarity of extreme events	Quantile-based extreme definition
	Temperature scale factor	1	0.8	1.2	Converts temperature change into event frequency change	Climate sensitivity of extreme events
Memory Dynamics	Memory window	2	0.5	5	Time horizon of climate experience integration	Experience timescale
	Memory retention factor	1	0.25	1.5	Controls persistence of remembered events	Memory retention duration
	Memory threshold	0.5	0	1	Minimum intensity required to influence perceived severity	Threshold for perception activation
Perception Process	Norm events	10	5	20	Baseline reference for perceived severity normalization	Scaling reference for event frequency
	Severity weighting	0.5	0	1	Weight of severity vs susceptibility in risk perception	Cognitive weighting parameter
	Extreme Intensity	0.5	0	1	Controls severity of individual extreme events	Physical intensity of events
	Intensity sensitivity	0.5	0	1	Nonlinear scaling of intensity on affected population	Amplification of physical impacts
	Perception delay	1	0.5	3	Time lag in updating perceived risk	Adjustment delay
Cognitive and emotional responses	SCA	0.5	0	1	Sensitivity of climate anxiety to perceived threat	Emotional responsiveness
	PAC	0.3	0.1	0.9	Belief in individual ability to act	Perceived self-capacity
	CAC	0.3	0.1	0.9	Belief in effectiveness of actions	Perceived response effectiveness

Table S2 First-order (S1) and total-order (ST) Sobol sensitivity indices of 13 human–climate system parameters across three emission scenarios (SSP1-2.6, SSP2-4.5, SSP5-8.5) and two time horizons (2050 and 2100). Parameters are grouped into four functional components of the coupled human–climate system: (i) cognitive adjustment and emotional response (PAC, CAC, SCA); (ii) mechanisms of memory (memory threshold, memory window, memory retention factor); (iii) processes of risk perception (extreme intensity, intensity sensitivity, norm events, severity weighting, perception delay); and (iv) characteristics of extreme events (extreme definition threshold, temperature scale factor). S1 represents the first-order (direct) contribution of each parameter to temperature variability, while ST captures both direct and interaction effects. Values are reported as mean sensitivity indices rounded to two decimal places. Values reported as 0 correspond to near-zero estimates (typically |value| < 0.005).

SSP126				
Parameter	**S1 (2050)**	**ST (2050)**	**S1 (2100)**	**ST (2100)**
PAC	0.41	0.51	0.39	0.47
CAC	0.41	0.51	0.4	0.47
SCA	0.02	0.06	0.02	0.1
Severity weighting	0.01	0.05	0.01	0.07
Memory window	0.01	0.04	0.01	0.05
Memory retention factor	0.01	0.03	0.01	0.04
Norm events	0.01	0.02	0.01	0.02
Extreme intensity	0	0.01	0.01	0.02
Temperature scale factor	0.01	0.01	0.01	0.01
Intensity sensitivity	0	0	0	0
Extreme threshold	0	0	0	0
Perception delay	0	0	0	0

Memory threshold	0	0	0	0

SSP245

Parameter	S1 (2050)	ST (2050)	S1 (2100)	ST (2100)
PAC	0.36	0.48	0.29	0.41
CAC	0.37	0.49	0.31	0.41
SCA	0.05	0.09	0.11	0.2
Severity weighting	0.02	0.09	0.02	0.07
Memory window	0.02	0.06	0.01	0.08
Memory retention factor	0.01	0.04	0.01	0.04
Norm events	0.01	0.03	0.01	0.03
Extreme intensity	0.01	0.01	0.01	0.02
Temperature scale factor	0	0.01	0	0.01
Intensity sensitivity	0	0	0	0.01
Extreme threshold	0	0	0	0
Perception delay	0	0	0	0
Memory threshold	0	0	0	0

SSP585

Parameter	S1 (2050)	ST (2050)	S1 (2100)	ST (2100)
PAC	0.31	0.46	0.23	0.38
CAC	0.34	0.46	0.27	0.36
SCA	0.03	0.12	0.22	0.34
Severity weighting	0.03	0.1	0.01	0.05
Memory window	0.03	0.06	0.03	0.08
Memory retention factor	0.01	0.04	0	0.04
Norm events	0.01	0.03	0.01	0.02
Extreme intensity	0	0.02	0.01	0.01
Temperature scale factor	0	0.01	0	0.01
Intensity sensitivity	0	0	0	0
Extreme threshold	0	0	0	0

Perception delay	0	0	0	0
Memory threshold	0	0	0	0

Table S3 Scenario-level contribution of key behavioral drivers to total-order (ST) sensitivity of temperature change across emission pathways (SSP1-2.6, SSP2-4.5, SSP5-8.5) and time horizons (2050 and 2100). PAC, CAC, and SCA denote the three dominant behavioral parameters. “Top-6 ST sum” represents the cumulative total-order sensitivity of the six most influential parameters (PAC, CAC, SCA, memory window, memory retention factor and severity weighting) within each scenario-year combination. “Share (%)” indicates the proportion of total sensitivity explained by these six parameters relative to the full set of 13 parameters. Values are rounded to two decimal places.

Scenario	**Year**	**PAC**	**CAC**	**SCA**	**Top-6 ST sum**	**Share (%)**
SSP1-2.6	2050	0.48	0.49	0.06	1.16	97.1
SSP1-2.6	2100	0.48	0.49	0.1	1.24	95.9
SSP2-4.5	2050	0.48	0.49	0.09	1.24	95.7
SSP2-4.5	2100	0.41	0.41	0.2	1.20	94.4
SSP5-8.5	2050	0.46	0.46	0.12	1.24	95.0
SSP5-8.5	2100	0.38	0.36	0.34	1.24	96.4

Table S4 Random forest variable importance of key behavioral parameters across three emission scenarios (SSP1-2.6, SSP2-4.5, SSP5-8.5) and two time horizons (2050 and 2100). Values represent %IncMSE, indicating the increase in mean squared prediction error when each parameter is permuted; higher values indicate greater importance of the parameter in explaining variability in projected temperature change. The analysis is performed for six key behavioral drivers: PAC, CAC, SCA, severity weighting, memory window, and memory retention factor. "SCA share (%)" denotes the proportion of total importance attributed to SCA, while "PAC+CAC+SCA (%)" represents the combined contribution of the three primary behavioral drivers relative to the total importance of the six-variable set. Values are reported as mean importance scores.

Parameter	**SSP126 2050**	**SSP126 2100**	**SSP245 2050**	**SSP245 2100**	**SSP585 2050**	**SSP585 2100**
PAC	605.95	627.3	656.67	585.47	608.71	568.18
CAC	644.15	629.18	604.78	572.8	581.82	508.74
SCA	490.68	542.75	638.85	768.56	642.6	756.28
Severity weighting	392.68	359.47	437.48	324.36	459.09	219.7
Memory window	120.52	131.1	150.14	146.85	162.71	109.88
Memory retention factor	111.96	114.08	134.08	129.33	143.95	100.77
SCA share (%)	20.74%	22.58%	24.36%	30.41%	24.73%	33.41%
PAC+CAC+SCA (%)	73.58%	74.85%	72.48%	76.24%	70.54%	80.99%